Digest Journal of Nanomaterials and Biostructures Vol. 9, No. 3, July – September 2014, p. 1241 - 1247

EFFECTS OF PROCESS PARAMETERS ON GROWTH OF METAL PARTICLES BY ATMOSPHERIC PRESSURE PLASMA JET

A. LAZEA-STOYANOVA[a,*], M. ENCULESCU[b], S. VIZIREANU[a], V. MÃRÃSCU[a], G. DINESCU[a]
[a]*National Institute for Laser, Plasma and Radiation Physics, 409 Atomiştilor street, 77125 Mãgurele, Bucharest, Romania*
[b]*National Institute of Materials Physics, 105bis Atomiştilor street, 77125 Mãgurele, Bucharest, Romania*

In this paper we report a procedure of growing metallic particles at atmospheric pressure by using a radiofrequency plasma jet, operated in inert gaseous atmosphere (argon). Iron metallic particles are manufactured, with sizes in the range of hundreds of nm up to a few microns, having as metal source the electrodes of the plasma jet discharge. The obtained particles are characterized with respect to their shape, size, morphology and size distribution. An emphasis is put on the relationship between the particle size distribution and process parameters, namely the substrate to nozzle distance and applied radiofrequency power.

(Received February 3, 2014; Accepted September 29, 2014)

Keywords: RF plasma jet; Metal particles; Particle growth

1. Introduction

Metal particles (MPs) have received special attention due to their specific physical properties. Tailored characteristics (size, internal structure, morphology, composition, shape, surface properties) made them suitable for many sectors of science and technology. Applications ranging from metallurgy, optics, catalysis, medicine, consumer electronics, sensors, solid fuels cells and up to environmental applications, are usually envisaged [1, 2, 3]. Conversely, particles can have detrimental effects, for example in semiconductor industry they can compromise the quality of chips, or in fusion technology the dust formed by walls erosion may incorporate significant amounts of tritium, thus limiting the long term operation of fusion machines.

Having in mind the importance of MPs it is understood the high interest for developing methods to produce particles, as well as to control their size, structure, morphology, composition, shape and surface properties. Various synthesis procedures were reported [4, 5, 6, 7, 8], using chemical or physical routes. Among many generation methods, gas-phase processes have the largest control possibilities and, therefore, such a process was chosen for our study. As concerning the procedures based on plasmas mostly low pressure processes were studied, using decomposition of metal containing precursors (plasma chemical route), or sputtering, evaporation and condensation of pure metals (plasma physical route) [7, 9]. In addition, last period was marked by reporting of processes using plasmas operated in contact with liquids [4, 5, 10, 11].

The novelty of the process presented here consists in using an atmospheric pressure plasma [12]. In order to obtain metallic particles a 13.56 MHz radiofrequency (RF) plasma jet was used. The electrodes of the plasma jet discharge (RF electrode and the nozzle) were made from stainless steel, representing the solid source of the material used for particle synthesis. Stainless steel was chosen due to the fact that iron particles have various uses ranging from catalytic, magnetic up to environmental applications [3, 4, 13]. The experiments revealed the successful fabrication of iron particles, of nm un to few microns in size. The influences of the plasma parameters (RF power, substrate-to-nozzle distance) upon the particle characteristics are studied.

* Corresponding author: andrada@infim.ro

The produced particles were investigated by Scanning Electron Microscopy (SEM) and Energy Dispersive X-ray Spectroscopy (EDX). The particles densities, and their size distributions could be modified by selecting the appropriate operating plasma parameters.

2. Experimental

In order to obtain metal particles we have used a versatile 13.56 MHz RF discharge configuration, consisting of an RF electrode and nozzle, described elsewhere [14]. A schematic drawing of the set-up is presented in Figure 1 - a). It consists of a plasma jet source, which can be operated at low, intermediate or atmospheric pressure, as described in detail in Ref. [12]. The electrodes were made from stainless steel (70% Fe, 21% Cr and 9% other metals) commercially known as AISI 304. The source generates a plasma jet which develops in a closed expansion chamber. A capillary mounted on the exhaust pipe is used to prevent the backflow of ambient air into the processing region.

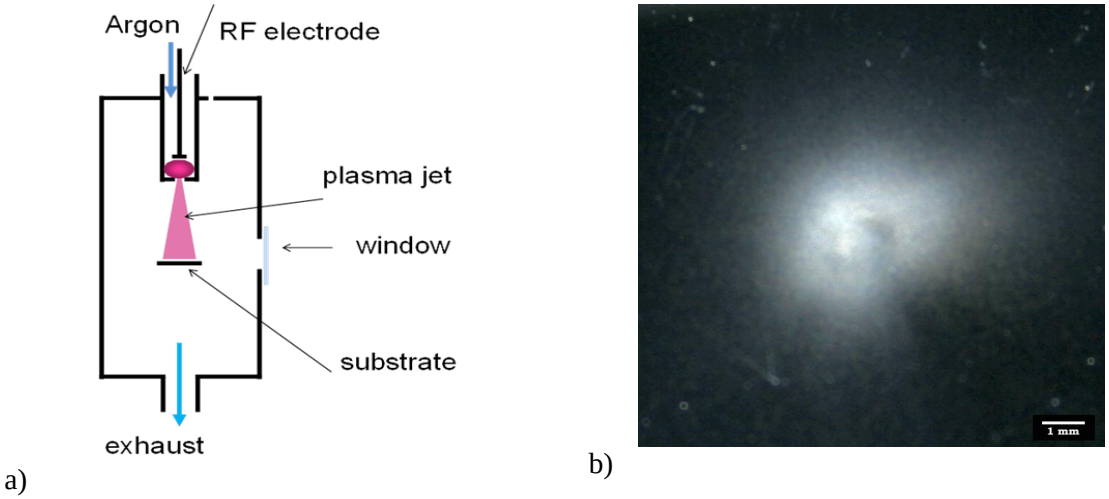

Fig. 1. a) Schematic drawing representing the experimental set-up; b) Image of the plasma deposited spot onto the Si substrate using 100 W and 6 mm substrate-to-nozzle distance.

The stainless steel grounded nozzle had a 2 mm central hole (nozzle). The used gas was argon (grade 6.0) with a total mass flow rate of 1500 sccm. The RF plasma power was varied between 50 W up to 200 W. The process designated pressure was kept constant at a value of 1040 mbar. In the expansion chamber, across the plasma jet a silicon substrate was placed. The substrate position with respect to the nozzle exit was variable, from 2 to 10 mm. After one hour operation time, deposits were collected on substrates.

Figure 1 - b) presents the image of a deposit, as recorded by a photo camera. It appears like a spot, with a size of a few mm, approximately equal with the plasma jet diameter. Such deposits were analysed by a SEM instrument (FEI Inspect S50) using 20 kV acceleration voltage. The elemental composition of the deposits was estimated with the EDX technique using a EVO 50 Zeiss SEM apparatus, equipped with a Quantax Bruker 200 X-ray detector. Additionally, optical emission spectroscopy analyses (OES) of the argon plasma were obtained using a quartz fiber (200 μm diameter), a Horiba Jobin Yvon imaging spectrograph (0.1 nm resolution) and a ANDOR IDus CCD camera.

3. Results and discussions

A typical optical emission spectrum during the synthesis of metal particles is shown in Figure 2. One can notice from the figure 2 - a) that the most significant lines are seen between 700 and 1000 nm, and correspond to the Ar I signature [15-17]. An observation that was expected since the used plasma gas was argon. Less intense are the lines corresponding to O I, NO, OH and NH species. Their presence might be due to the impurities into the plasma gas and/or to the leaks of the outside atmosphere into the chamber. Figure 2 - b) represents a zoom of the same OES spectrum, in the range 200 nm up to 300 nm. In this case, the spectrum is dominated by the line corresponding to Fe I, and less intense are the lines describing the presence of NO and OH species. The iron presence is to be expected since the RF electrodes are made out of stainless steel, containing 70% iron, and these analyses denote a sputtering/evaporation of the electrode material.

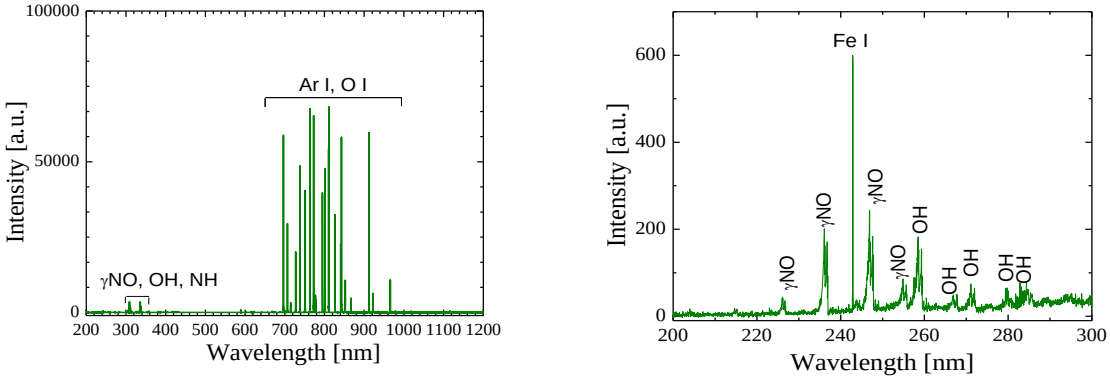

a) b)

Fig. 2. OES spectrum of RF plasma jet, operating in Ar, taken during metal nanoparticle growth (at 100 W and 10 mm substrate-to-nozzle distance) for various wavelengths ranges: 200-1200 nm (a) and 200-300 nm (b).

Representative SEM images of the deposited material collected on a substrate placed at 6 mm from the nozzle are shown in Figure 3 - a), b). Spherical particles of various sizes are observed. From the SEM images it can be noticed that the morphologies of the particles, regardless of their sizes, are similar, and their surface quite smooth. Apparently, few particles present facets, suggesting a crystalline structure.

As concerning the composition of the particles, the EDX mapping, shown in Figure 3 - c), clearly point out that mainly iron (Fe) is the particle's compositional element (blue colour), regardless of their size. Except from Fe, at the sample's level some traces of carbon (C) were also identified (red colour). The presence of small quantities of C may be attributed either due to the C contained into the stainless steel bulk material either due to the contamination coming from the deposition chamber, or both.

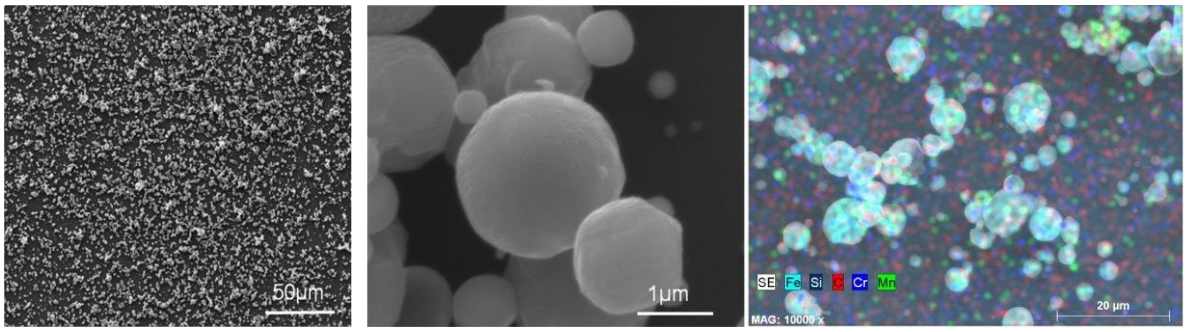

a) *b)* c)

Fig. 3. Images of the metallic nanoparticles obtained using 1040 mbar, 100 W and 6 mm substrate-to-nozzle distance: SEM investigations (a,b) and EDX mapping (c).

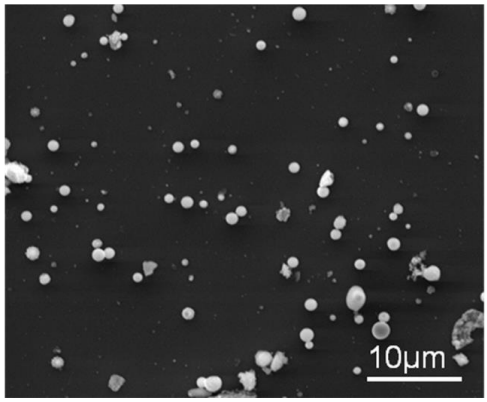

a)

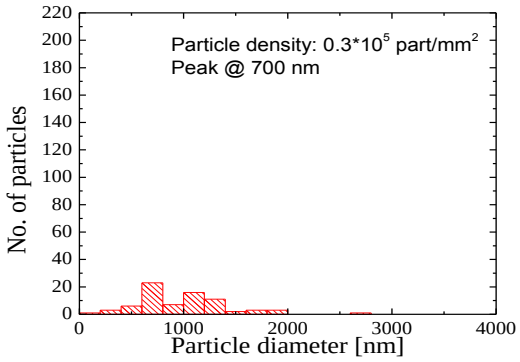

b)

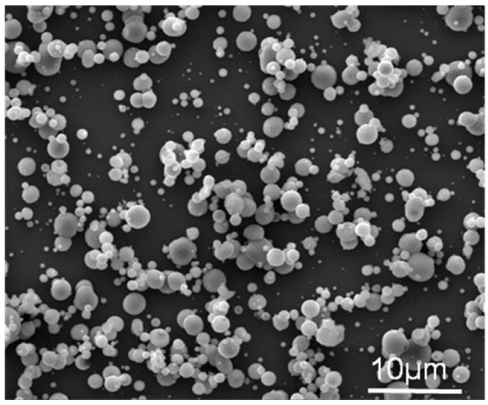

c)

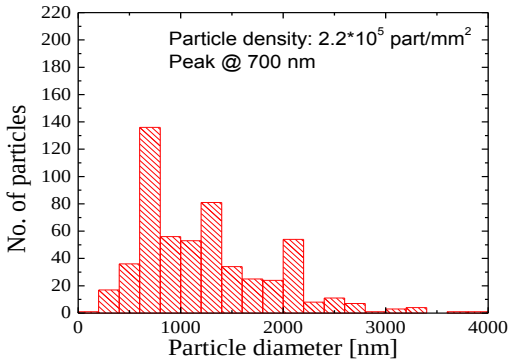

d)

f)

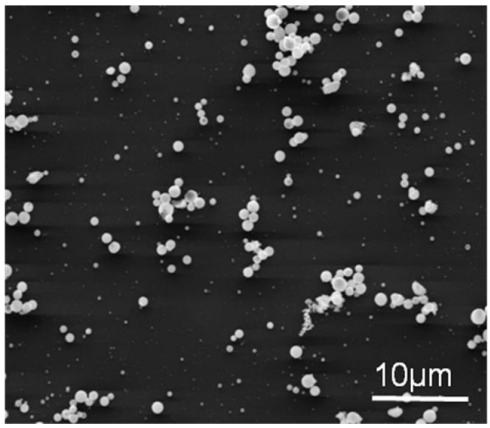

e)

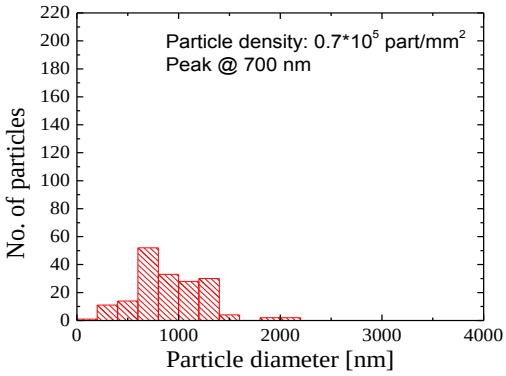

Fig. 4. SEM images (left hand side column) and particle size distributions graphs (right hand side column) for samples grown using 100 W, 1040 mbar and various substrate-to-nozzle distances: 2 mm (a, b), 6 mm (c, d) and 10 mm (e, f).

Additionally, the obtained SEM images were analysed via homemade software, in order to determine the particles sizes distributions. Figure 4 presents SEM images and the specific distributions for the iron particles obtained at various substrate-to-nozzle distances: 2 mm, 6 mm and 10 mm, respectively. It must be mentioned that all the size distributions were evaluated from micrographs with identical areas, of 2500 μm^2, chosen from the central part of the deposited spot. Regardless of the substrate-to-nozzle distance, one can notice that the particle distribution is large, showing that particles with diameters in the range 0.3-3 μm were obtained. However, over this large distribution a peak at about 700 nm is noticed for all three substrate-to-nozzle distances. This aspect suggests that, possibly, a method of producing particle with narrow size distribution can be developed by further process optimization.

Moreover, from the dependences of the particles size distributions upon the substrate-to-nozzle distance further remarks can be outlined. A first observation from the graphs presented in Figure 4 (b, d, f) is that at short substrate-to-nozzle distance, namely 2 mm, the generated particles had a density of $0.3x10^5$ particles/mm^2. At medium distances (6 mm) their density increases, reaching $2.2x10^5$ particles/mm^2, whereas for long distances (10 mm) the density slightly decreases to $0.7x10^5$ particles/mm^2. This behaviour is well correlated with SEM images shown in Figure 4 (a, c, e). Hence, we can draw the following conclusion: by adjusting the substrate-to-nozzle distance is possible to change the density of the obtained particles.

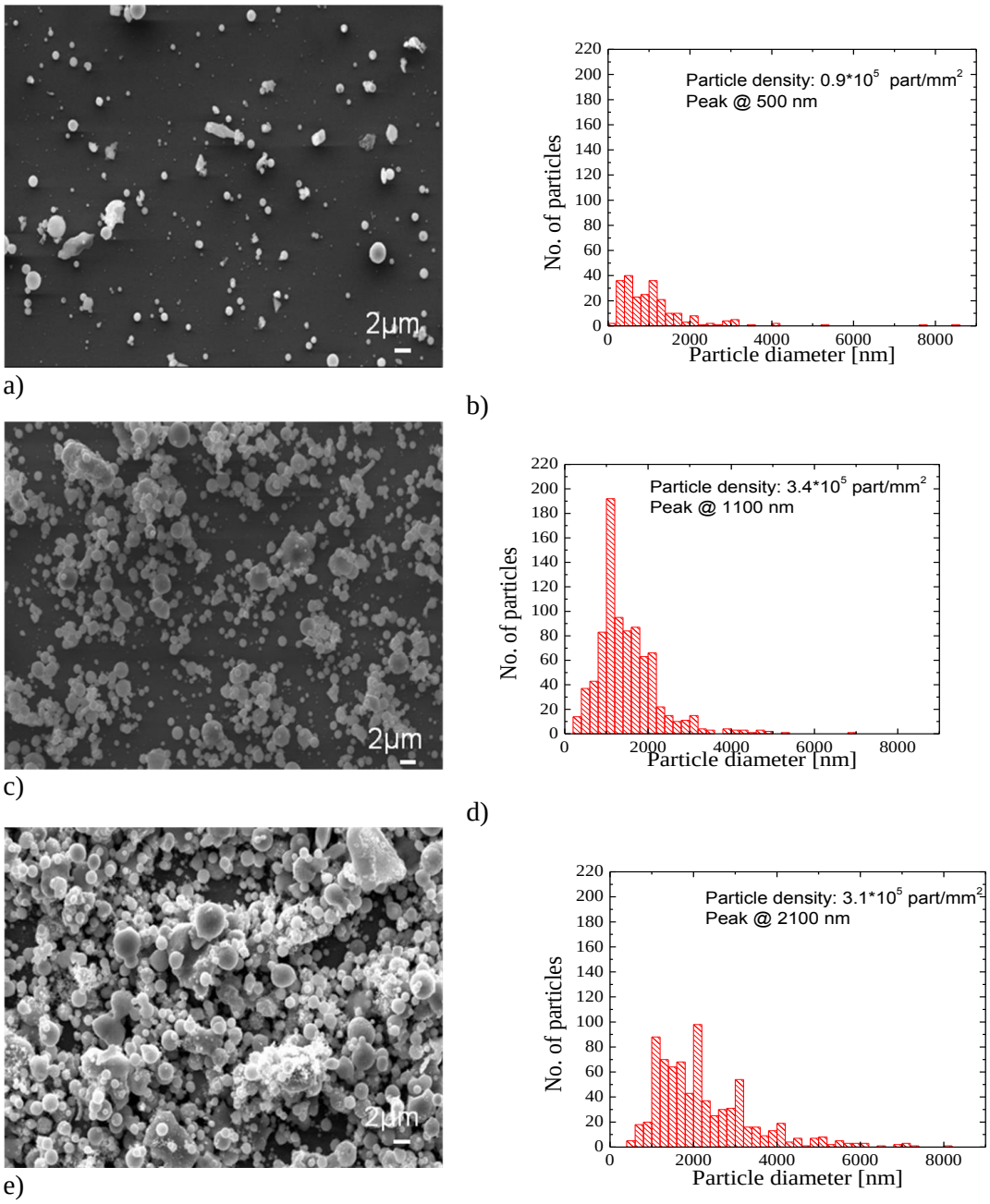

Fig. 5. SEM images (left hand side) and particle size distributions graphs (right hand side) for samples grown using 6 mm substrate-to-nozzle distance, 1040 mbar and various RF powers: 50 W (a, b), 150 W (c, d) and 200 W (e, f).

Figure 5 presents SEM images and their specific distributions for iron particles obtained at different RF powers: 50 W, 150 W and 200 W, respectively. For low RF power (figure 5 - a, b) the particle density is $0.9x10^5$ particles/mm^2. A further increase of the power, up to 150 W as presented by figure 5 - c, d, will determine an increase of the particle density up to $3.4x10^5$ particles/mm^2. Moreover, this trend is also seen in the case of particle peak, which shifts from 500 nm at 50 W up to 1100 nm at 150 W. However, for very high RF powers (200 W) particles start to lose their spherical shape and a noticeable increase in the particle diameter is seen (Figure 5 - e, f). In this case a density of $3.1x10^5$ particles/mm^2 was measured. This behaviour might be explained by the fact that at higher RF power the metallic particles start to agglomerate probably due to the insufficient cooling of the metallic material sputtered/evaporated from the electrodes.
As a result of changing the RF power, the following conclusion can be drawn: by increasing the plasma power, from 50 W up to 150 W, it is possible to change the size and the surface density of the obtained particles. However, for high powers, the particles start to lose their spherical shape and drastically increase in size.

4. Conclusions

We report a novel method for synthesis of iron particles by using an atmospheric pressure plasma jet sustained by a RF discharge operated in argon. The gas-phase process had as metal source bulk material, namely the stainles steel electrodes of the discharge. The iron presence in the atmospheric pressure plasma jet was clearly shown by optical emission spectroscopy. The process of electrodes erosion requires further investigation: sputtering at atmospheric pressure is low due to the collisional plasma regime that prevents the ions from reaching high energies, therefore evaporation should be active. The atoms supplied by the plasma process are cooled during argon plasma expansion leading to particles nucleation and growth.

The particles size distribution is generally large. The dependence of distribution upon substrate-to-nozzle distance and upon RF power was investigated. Regardless of the distance, at a constant power of 100 W, the maximum of particle size distribution is preserved at about 700 nm. However, the change of substrate position lead to modification of the particle surface density, the maximum density being obtained at an optimum distance of 6 mm. In respect to the dependence of the RF power, at a fixed position of 6 mm, the power increase from 50 W up to 150 W led to the displacement of the maximum of particle size distribution towards higher size values from 500 nm up to 2100 nm. In addition, besides the drastically increase in size, the particles start losing their spherical shape.

Acknowledgements

This work supported by project number C1-05 within the framework of cooperation between IFA, Romania and CEA, France and the project IDEI PN-II-ID-PCE-2012-4-0629.

References

[1] I. Sevonkaev, V. Privman, D. Goia, J Solid State Electrochem. **17**, 279 (2012).
[2] R. Bonelli, PhD Thesis, Univ. Bologna, 1-151 (2010).
[3] Jyoti Kishen Kumar and Aniruddha Bhalchandra Pandit, Drinking Water Disinfection Techniques, by CRC Press - 270 Pages, ISBN 9781439877401 (2012).
[4] D. Mariotti, R. M. Sankaran, J. Phys. D: Appl. Phys. **43**, 323001 (2010).
[5] D. Mariotti, R. M. Sankaran, J. Phys. D: Appl. Phys. **44**, 174023 (2011).
[6] K. Ostrikov, U. Cvelbar, A. B. Murphy, J. Phys. D: Appl. Phys. **44**, 174001 (2011).
[7] H. Bonnemann, R. M. Richards, Eur. J. Inorg. Chem. 2001, **10**, 2544 (2001).
[8] O. V. Kharissova, B. I. Kharisov, Recent Pat. Nanotechnol. **2(**2), 103 (2008).
[9] T. A. Kareem, A. A. Kaliani, Ionics **18**, 315 (2012).

[10] W.-H. Chiang, C. Richmonds, R. M. Sankaran, Plasma Sources Sci. Technol. **19**, 034011 (2010).
[11] W. G. Graham, K. R. Stalder, J. Phys. D: Appl. Phys. **44**, 174037 (2011).
[12] M. Teodorescu, M. Bazavan, E.R. Ionita, G. Dinescu, Plasma Sources Sci. Technol. 21, 055010 (2012).
[13] D. L. Huber, Small **1(**5), 482 (2005).
[14] G. Dinescu, B. Mitu, E. Aldea, M. Dinescu, Vacuum **56(**1), 83 (2000).
[15] R. Mavrodineanu, H. Boiteaux, Flame Spectroscopy, J. Wiley&Sons, 64-20088 (1965).
[16] http://www.pmp.uni-hannover.de/cgi-bin/ssi/test/kurucz/sekur.html
[17] http://www.nist.gov/pml/data/asd.cfm